

HEAVY METALS REMOVAL BY USING MAGNETIC IRON OXIDE/TiO₂ NANOCOMPOSITE FOR WASTEWATER TREATMENT IN 10TH OF RAMADAN CITY, EGYPT

El-Sayed, Magdy H. and Yasser A.M. Abdilhady*

Egyptian Desalination Research Center of Excellence (EDRC), Water Treatment and Desalination Unit, Desert Research Center, Cairo, Egypt

*E-mail: Yasser_vip6@hotmail.com

Super-paramagnetic iron oxide nanoparticles with appropriate surface chemistry exhibit many interesting properties that can be exploited in a variety of water treatment applications. These applications require the magnetic nanoparticles (MNPs) to have high magnetization values and particle size smaller than 100 nm. This paper discussed the experimental details for preparation of mono-disperse titania coated iron MNPs by chemical co-precipitation method and micro-emulsion with different surfactants. These experimental preparation processes were vital to determine the optimum pH, initial temperature and sonication time in order to obtain the iron oxide MNPs coated TiO₂-anatase with small particle size and size distribution that is needed for water treatment applications. The nanoparticles were characterized by FT-IR, XRD, VSM and SEM. Removal efficiency of iron and chromium in Sewage water using the prepared MNPs after treatment were observed to be 98.66 and 92.38%, respectively. Removal efficiency of iron and chromium in industrial wastewater were observed to be 98.74 and 99.89%, respectively. Removal efficiency of iron and chromium in synthesized solution after treatment were observed to be 92.56 and 80.69%, respectively. Reduction % of total nitrogen, nitrate and phosphate in sewage water of 10th Ramadan city after treatment were observed to be 33.33, 100 and 53.44%, respectively. Reduction % of total nitrogen, nitrate and phosphate in industrial wastewater after treatment were observed to be 31.25, 56.64 and 100 %, respectively. Results of this study well demonstrate the efficiency of nanosized iron oxide-coated titanium oxide treatment of wastewater; upon 98-100% of inorganic pollutants such as iron, chromium, nitrate and phosphates could be removed.

Keywords: adsorption, iron and chromium removal, wastewater treatment, magnetic nanoparticles, titania iron magnetic nanocomposite, nitrogen-nitrate and phosphate removal

Heavy metals treatment from wastewater is of special concern due to their harmful damage to the environment. Water pollution by chromium is due to both, natural sources and man-made activities. Chromium is found in rocks, animals, plants, soils and in volcanic dusts and gases. Various industrial processes, which involve the use of Cr (VI), such as steel production, electroplating, leather tanning, nuclear power plants, textile industries, wood preservation, anodizing of aluminum, water-cooling and chromate preparation are sources for chromium pollution (Okuda et al., 1975; Ouki and Neufeld, 1997 and Altundogan, 2005). In Egypt, chromium level discharged in sewage water is 0.5 mg/L. In nature, chromium exists in two oxidation states, i.e., trivalent and hexavalent forms in aqueous systems. Also, magnetic nano-materials based composite adsorbents can be easily isolated from aqueous solutions for recycling or regeneration (Zhao et al., 2011). This method is essential to improve the operation efficiency and decrease the cost of wastewater treatment technique. Magnetite nanoparticles have attracted increasing research interest in the fields of catalysis and environmental remediation in recent years (Ngomsik et al., 2005). Magnetite nanoparticles possess not only strong adsorption/reduction activities, but also the property of being easily separated and collected by an external magnetic field (Booker et al., 1991 and Orbell et al., 1997). TiO₂ nanoparticles have important environmental, technological and biomedical applications (Goh et al., 2015). The adsorption performance depends mainly on the size and shape of the magnetic nanoparticles (MNPs). Synthetic method has an effective role for shape-controlled, highly stable, and mono-disperse metal oxide nano-materials studied during the last decade. Iron is one of the most widespread elements in the earth. The facileness of resource and ease in synthesis render nanosized ferric oxides (NFeOs) to be low-cost adsorbents for toxic metal sorption. Since elemental iron is environmentally friendly, risks of secondary contamination with treatment of NFeOs can be negligible. Maghemite (Fe₂O₃) nano-gels can be prepared by a sol-gel method, that is, adding NH₄OH solution to the mixture of FeCl₃ and FeCl₂ in the purified water deoxygenated and bubbled by nitro-gen gas. The prepared maghemite nanoparticles are expected to respond well to magnetic fields without any permanent magnetization. Nanosized magnetite is another important nano-material, which has effective removal efficiency of heavy metals and has strong magnetizing efficiency. Chemical co-precipitation has been widely used to prepare magnetite nanoparticles by adding alkaline solution containing ferrous and ferric (Tartaj et al., 2003 and 2005). In addition, nano-Fe₃O₄ will be oxidized to nano-iron oxide. The size of the resultant Fe₃O₄ or Fe₂O₃ hydrosols were considerably smaller than that reported in the literature (Pathak et al., 2003 and Chang and Chen, 2005) and no surfactants are needed to stabilize the sols. A decrease of specific saturation magnetization(s) value was observed when the nanoparticles were coated with surfactant. Scanning electron micrograph showed that the prepared

Fe₃O₄ nano-particle sol had an average diameter of 8.5 ± 1.3 nm, where needlelike Fe₂O₃ nanoparticles with lengths of 20–50 nm and widths of 4–6 nm are visible (Kang et al., 1996). For removal of heavy metals, nano Fe₃O₄ was commonly used as the magnetic core for composite sorbents (Warner et al., 2010). Nanosized titanium oxides anatase exhibit different chemical behavior, catalytic reactivity, and surface acidity based on their different surface planes. The nanoparticles were able to simultaneously remove multiple metals (Zn, Cd, Pb, Ni, Cu) from a solution of pH = 8. The aim of the present study is concerned with the preparation of new compounds by new technical methodology that have the ability to remove different contaminant of polluted wastewater by high reduction efficiency.

MATERIALS AND METHODS

1. Chemicals and Reagents

All chemical materials used in this study were provided from Merck and Sigma Aldrich Companies.

2. Experimental Procedure

2.1. Sol-gel route

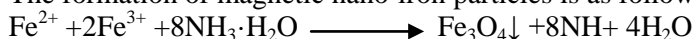
The sol-gel synthesized TiO₂ was obtained by dissolving titanium (IV) isopropoxide (TTIP) in absolute ethanol and distilled water then added to the solution in terms of a molar ratio of Ti: H₂O=1:4. Citric acid was used to adjust the pH and restrain the hydrolysis process of the solution. The solution was vigorously stirred for different reaction time in order to form sols. After aging for 24 h, the sols were transformed into gels. In order to obtain nanoparticles, the gels were dried under 100°C for 5 h to evaporate water and organic material to the maximum extent. Then the dry gel was sintered at 400°C for 3 h were subsequently carried out to obtain desired TiO₂ nano-crystalline.

3. Synthesis of Iron Oxide MNPs.

3.1. Sample preparation

The reagents used for the synthesis were ferric chloride hexa-hydrate (FeCl₃·6H₂O), ferrous chloride tetra-hydrate (FeCl₂·4H₂O), propylene glycol (CH₃CH(OH)CH₂(OH), sodium hydroxide (NaOH) and ammonium hydroxide (NH₄OH, 26% of ammonia). Sample A was synthesized by the co-precipitation method. A certain weight of ferric chloride was added to ferrous chloride molar ratio of Fe³⁺/Fe²⁺=2) and 150 ml of (NH₄OH, 26% of ammonia) with 300 ml of de-ionized water in a 500 ml flask. Finally, the MNPs product was separated by a centrifuge and washed twice with deionized water and ethanol. The obtained MNPs were dried at 100°C for 6 h (Cornell and Schertmann, 1991).

The formation of magnetic nano-iron particles is as following:



3.2. Sample characterization

FT-IR spectra were measured in a transmission mode on a spectrophotometer (Perkin Elmer Spectrum Version 10.03.09). Spectrum Two Detector LiTaO₃ was used for separating the solid and liquid during the preparation samples. The samples were mixed with KBr. The micrographs of prepared particles were obtained using a Scanning Electron Microscope using SEM Model Quanta 250 FEG (Field Emission Gun). The X-ray diffraction (XRD) pattern of TiO₂ and MNPs was obtained using a X-ray diffractometer Shimadzu model: A PAN analytical X-rays diffraction equipment model Xpert PRO with secondary monochromator, Cu-radiation ($\lambda=1.54\text{\AA}$) at 50 k.v., 40 M.A and scanning speed of 0.02°/sec. Magnetic properties of the particles were assessed with a vibrating-sample magnetometer (VSM, Homade 2 tesla). A magnet (Φ 17.5×20 mm, 5500 Oe) was utilized for the collection of magnetic particles. Basing on the results of measurements, coercivity, remenance and saturation of samples have been determined, from each powder sample a certain amount of sample has been portioned out, put into another container and weighed. The VSM measurements have been performed on every sample.

3.3. Examine adsorbents efficiency

Batch adsorption studies were performed by mixing 0.015, 0.025, 0.05, 0.1 gm of MNPs with 50 ml of the synthesized wastewater in a flask. For pH adjustment we used standard 0.1M HCl and 0.1M NaOH solutions. The solution mixture of MNPs was put with wastewater solution in sonicator for different time. After adsorption reached equilibrium, the adsorbent was conveniently separated via an external magnetic field and the solution was collected for metal concentration measurements. MNPs were washed thoroughly with deionized water to neutrality. The concentrations of metal ions were measured by a plasma-atomic emission spectrometer (ICP-AMS, Optima 3000XL, PerkinElmer) in accordance with the Standard Method. In order to obtain reproducible experimental results, the adsorption experiments were carried out at least 3 times.

3.4. Field measurements

In situ measurements of water samples location were carried out in the field using GPS model (Magellan Nave 5000 pro.) for the determination of latitudes and longitudes. Some physical and chemical characteristics of the collected water were determined by electrical conductivity meter, Jenway, model 470 (EC in $\mu\text{s}/\text{cm}$) for the collected water samples.

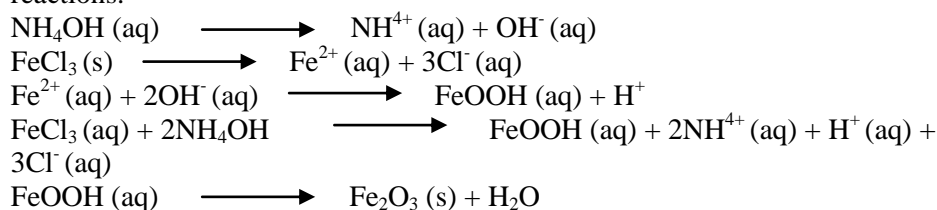
3.5. Laboratory analyses

The analyses include the determination of EC, TDS and pH. The minor, trace and soluble heavy metals and non metals are total nitrogen, NO³⁻, PO₄³⁻, B³⁺, Al³⁺, Fe³⁺, Mn²⁺, Co²⁺, Cu²⁺, Ni²⁺, Cr³⁺, Cd²⁺, Pb²⁺, Sr²⁺, V²⁺ and Zn²⁺.

RESULTS AND DISCUSSION

1. Mechanism of the Iron Oxide MNPs Formation

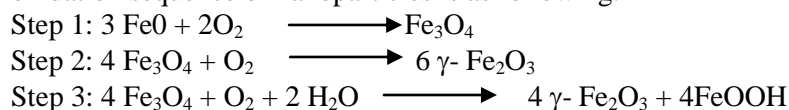
During the precipitation of Fe_2O_3 from Fe^{2+} and Fe^{3+} salts mixtures, two separate reactions could occur after addition of ammonium hydroxide to observe the precipitation of Fe_2O_3 MNPs. $\text{Fe}(\text{OH})_2$ and $\text{Fe}(\text{OH})_3$ formed at $\text{pH} > 8$ by the hydroxylation of the ferrous and ferric ions under anaerobic conditions. The iron oxide MNPs formation occurred with black precipitation. By reaching to end point of chemical reaction, formation of black precipitation was formed fastly with very high yielding of MNPs crystals. The FeCl_3 reacts with NH_4OH and forms FeOOH , which, upon heating, further produce into Fe^{2+} and OH^- ions, which consequently assists in the development of Fe_2O_3 ions according to the following chemical reactions:



Fe_2O_3 nuclei perform as building blocks for the development of final products. The Fe_2O_3 nuclei concentration enlarges, which escorts the construction of desired nano-particle products.



From observation and lattice parameter calculations, the proposed oxidation sequence of nanoparticles is as following:



2. Optimized Conditions for Synthesis of Iron Oxide MNPs

2.1. Effect of pH variation on particle size

The pH range during the synthesis of iron oxide NPs should be 8-11 with maintaining molar ratio of $\text{Fe}^{3+}/\text{Fe}^{2+}$ (2:1) under a non oxidizing condition. This study showed that the size of iron oxide MNPs reduce with the increase of solution pH when the pH is lower than 11, and also the particle size of iron oxide MNPs increased with the increase of solution pH when the pH is higher than 11 (Fig. 1 and 2). After increasing of the pH of the solution, the hydrolysis of Fe^{3+} occurred and $\text{Fe}(\text{OH})_3$ was generated in the first step. Then, $\text{Fe}(\text{OH})_2$ was generated as the pH of the reaction system increased, which was attributed to the hydrolysis of Fe^{2+} . Finally, Fe_3O_4 can just be formed as the pH of the solution is further increased. This result shows that the growth of Fe_2O_3 nucleus occurred when the pH of solution is

lower than 11, while the growth of Fe₃O₄ nucleus is easier to happen when the pH of solution is higher than 11 (Sun et al., 2006). The desired pH estimated was less than pH 11 where complete nucleation occurred.

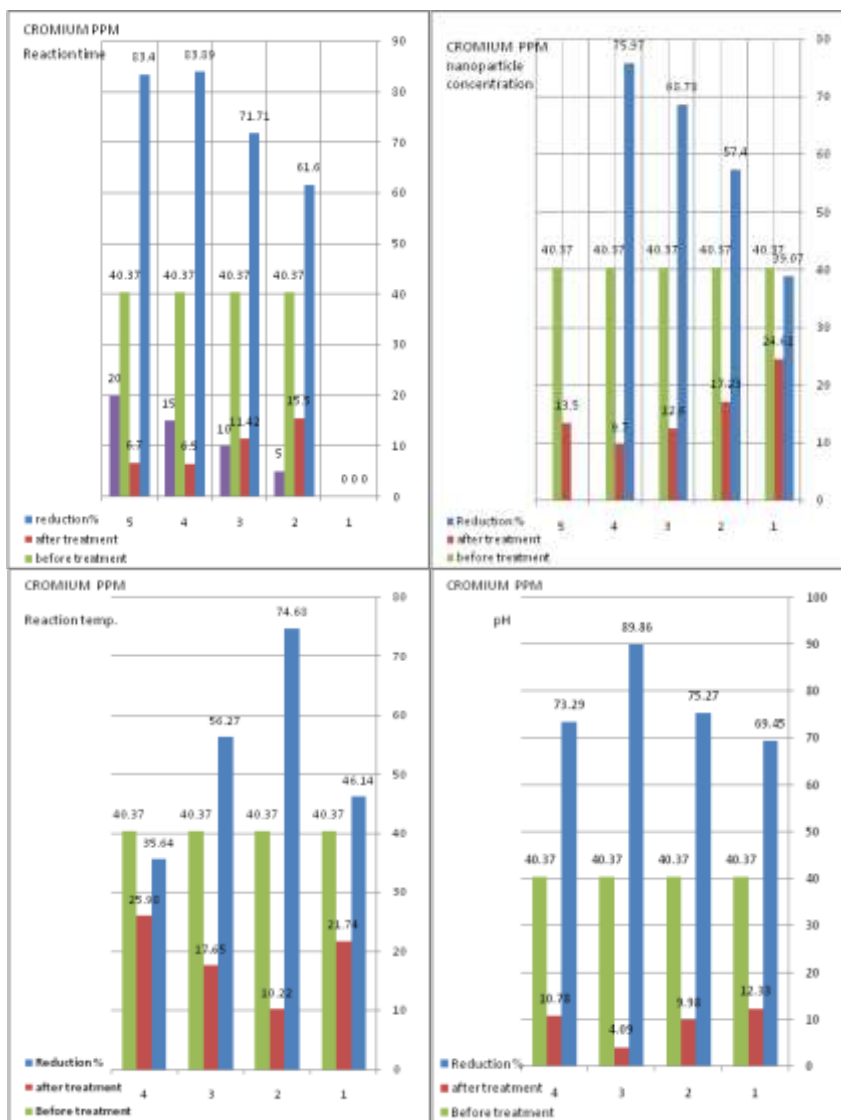


Fig. (1). Effect of different conditions on chromium concentration.

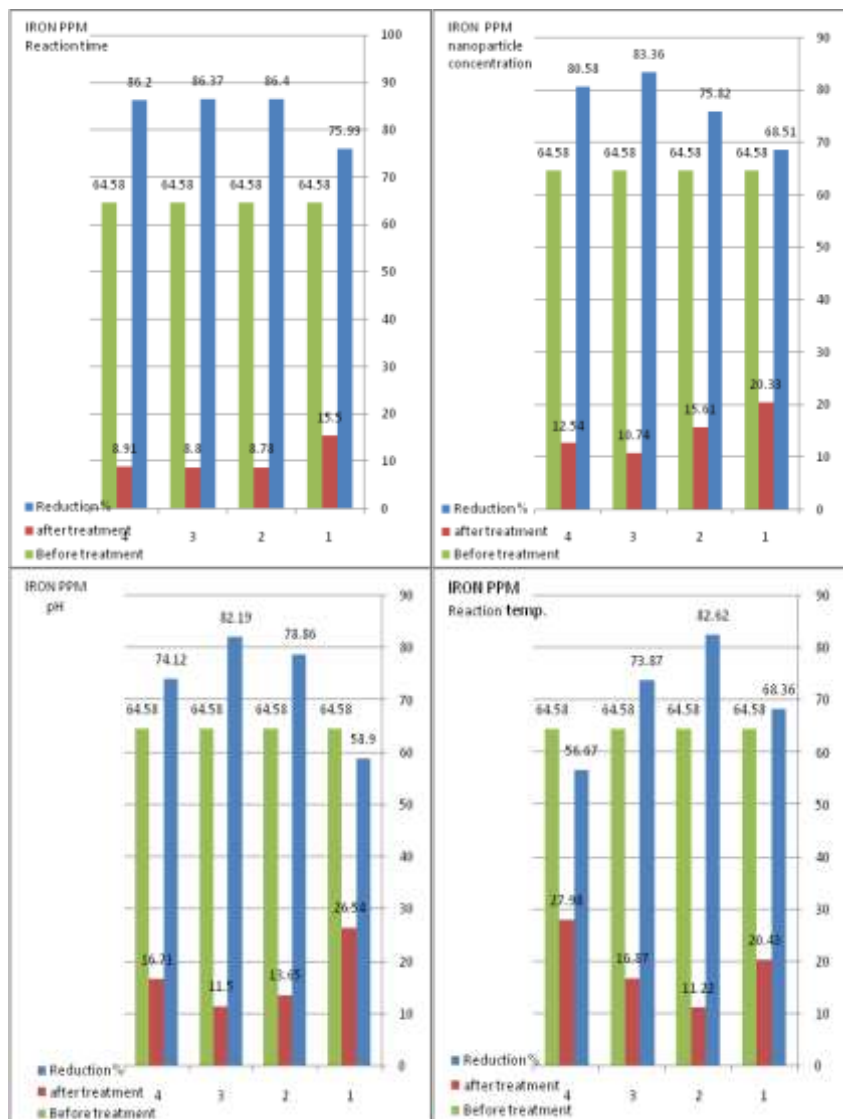


Fig. (2). Effect of different conditions on iron concentration.

2.2. Effect of sonication time on particle size

As the sonication time was increased, the average sizes of the iron oxide nanoparticles were decreased. The energy transferred to the suspension medium is also increased and the reaction solution can be dispersed into smaller droplets and the size is reduced. Another explanation for this reduction was that the anomalous diffusion of particles at higher degree of agitation reduced the growth kinetics of the particles, and resulted in the

smaller sized particles. Mean diameters of iron oxide nanoparticles was 21.1 nm by NICOMP/GAUSSIAN distribution analysis.

2.3. Particle size analysis of iron nano-composite with TiO₂

As shown in Fig. (3) the nanoparticle intensity weighting was 89.4 nm, volume weighting was 39.2 nm and number weighting was 21.1 nm.

Fig. (4) shows that the mean diameter of nanocomposite material ranges around 21.1 nm. This reading means that the obtained results of reduction percent of prepared nano iron composite depends mainly on the size and shape with availability of dispersion percent in solution.

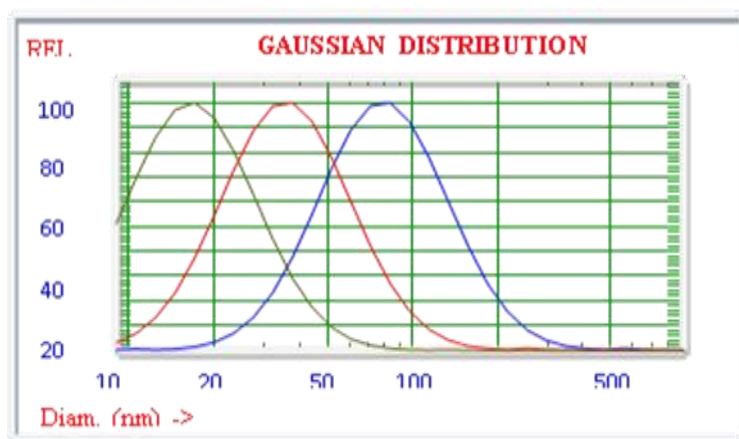


Fig. (3). Particle size distribution of iron nano-composite by Gaussian distribution.

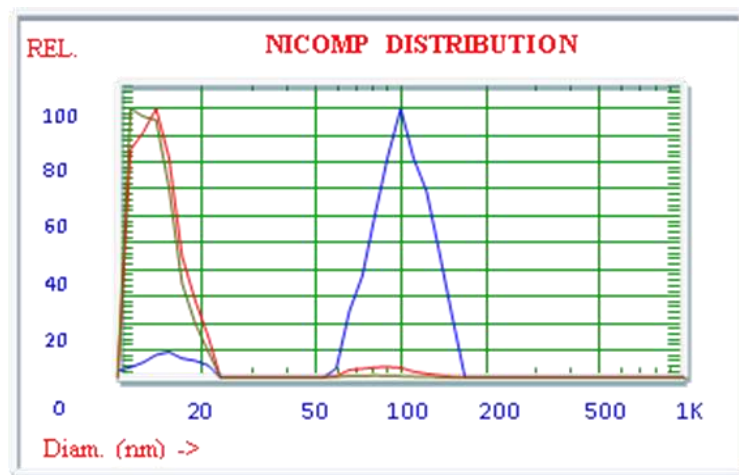


Fig. (4). Particle size distribution of iron nano-composite by NICOMP distribution.

3. Characterization of the Adsorbents

3.1. Infrared spectroscopy (FTIR)

Data in Fig. (5) show that peaks at 530 cm^{-1} corresponding to the Fe-O vibration are related to the magnetite phase and two absorption peaks at $2,924$ and $2,854\text{ cm}^{-1}$ were attributed to the asymmetric and symmetric CH_2 stretching, respectively (Shen et al., 2009). The intense peak at $1,710\text{ cm}^{-1}$ was due to the overlapping of the absorption bands of the carboxyl groups and the double bonds of surfactant. The results of the significant shift of these specific peaks to the lower frequency indicated that the hydrocarbon chains in the monolayer surrounding the nanoparticles were in a closed-packed, crystalline state (Mahdavi et al., 2013). The bands due to C-O stretching mode were merged in the very broad envelope centered on 1268 and 1007 cm^{-1} arising from C-O, C-O-C stretches and C-O-H bend vibrations of iron oxide NPs in surfactant. Also, the aliphatic C-H stretching, in 1413 and 1344 cm^{-1} were due to C-H bending vibrations. The broad band centered at $500\text{-}600\text{ cm}^{-1}$ is likely due to the vibration of the Ti-O bonds in the TiO_2 lattice (Gao et al., 2003). The broad peak in 407 cm^{-1} related to iron oxide NPs banding, therefore, the FT-IR spectra showed the existence of van der Waals interactions between the chain of TiO_2 and iron oxide NPs. The IR band at 3455 cm^{-1} can be assigned to the stretching modes of surface H_2O molecules or to an envelope of hydrogen-bonded surface OH groups. The IR band at 3144 cm^{-1} can be assigned to the OH stretching mode in the goethite structure. The IR band at 1643 cm^{-1} is close to the position of H_2O bending vibrations. In the spectrum of the pure pectin sample, the peaks at 3253 cm^{-1} and 2946 cm^{-1} represent secondary hydroxyl groups and carboxylic hydroxyl groups, respectively.

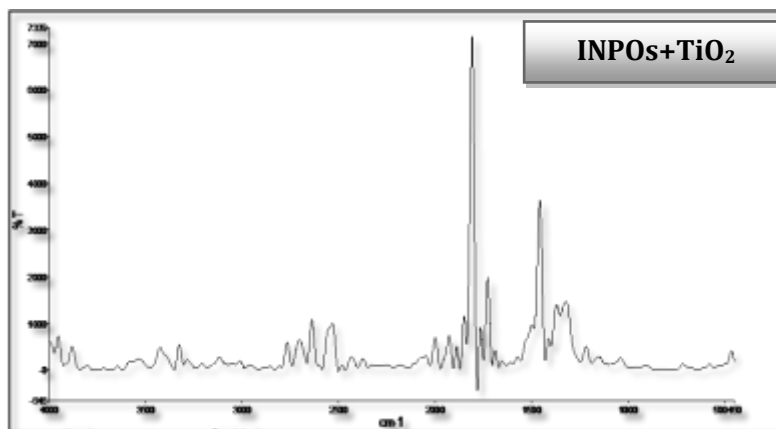


Fig. (5). FTIR spectra of the iron oxide nanoparticles composite with TiO_2 .

3.2. X-ray diffraction analysis (XRD)

Fig. (6) shows a series of characteristic peaks in the XRD pattern at 2θ of 23.9° , 33.2° , 35.5° , 40.9° , 49.5° and 54.1° corresponding to the diffractions of crystal faces of Fe_2O_3 and Fe_3O_4 spinel structure. A series of characteristic peaks were observed in the XRD pattern at 2θ of 25.5° and 38.2° corresponding to the diffractions of crystal faces of TiO_2 anatase spinel structure. The positions and relative intensities of the reflection peak of Fe_3O_4 and Fe_2O_3 MNPs agree with the XRD diffraction peaks of standard Fe_2O_3 samples (Mahdavi et al., 2007), indicating that the black-colored magnetic powders are mixture of hematite and magnetite nanoparticles. Sharp peaks also suggest that the Fe_3O_4 and Fe_2O_3 nanoparticles have well crystallized structure. Peak broadening observed is consistent with the small particle size. It was found that the magnetite crystallites could be well indexed to the inverse cubic spinel structure of Fe_3O_4 .

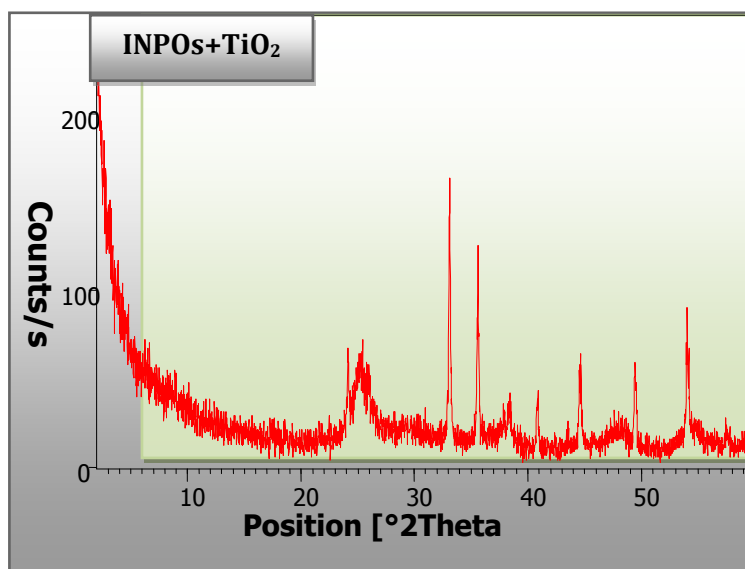


Fig. (6). XRD pattern of iron oxide MNPs coated with TiO_2 .

3.3. Scanning electron micrograph (SEM)

Fig. (7) shows the SEM images for the iron oxide MNPs, which confirms that the Fe_3O_4 MNPs are cubic and highly uniform in size with spherical round of Fe_2O_3 MNPs. Also, SEM image shows the TiO_2 particles coat the core magnetic iron oxide nanoparticles with homogenous distribution approximately.

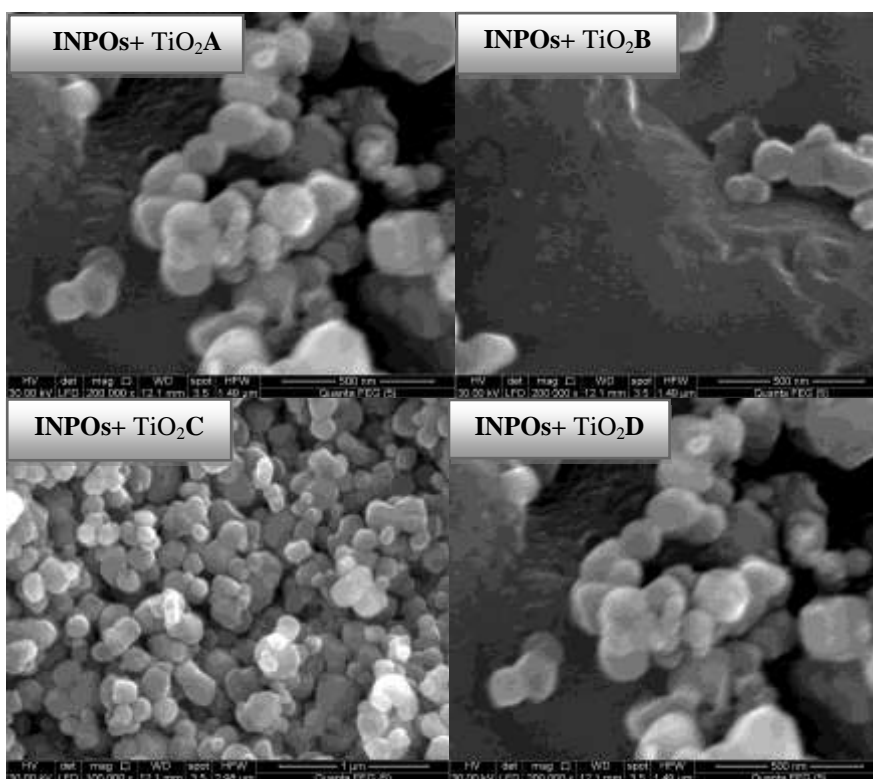


Fig. (7). SEM micrograph of TiO_2 -anatase coated iron oxide MNPs.

3.4. Vibrating sample magnetometer (VSM)

The magnetization curves measured at room temperature for iron oxide MNPs coated with TiO_2 -anatase are showed in Fig. 8 and 9. There was no hysteresis in the magnetization of sample, suggesting that produced magnetic particles are superparamagnetic. This can be attributed to the small size of NPs (Pradhan et al., 2006). On the other hand, when the magnetic component size of the particles is smaller than critical size, the particles will exhibit super paramagnetism (Guo et al., 2010). The saturation magnetization value was measured to be 81.40 emu g^{-1} for Fe_3O_4 . The high saturation magnetization of pure Fe_3O_4 indicated the good crystal structure. The saturation magnetization values of TiO_2 coated Fe_3O_4 was smaller than the value for the pure magnetite nanoparticles, therefore the saturation magnetization was reduced after coating of TiO_2 onto the surface of Fe_3O_4 and Fe_2O_3 MNPs. This was due to the existence of diamagnetic shell surrounding the magnetite nanoparticles, which quench the magnetic moment (Qu et al., 2010). However, both of them showed super paramagnetic behaviors, indicating that magnetite and hematite nanoparticles were incorporated in the composite particles, which exhibited no remanence effect from the hysteresis loops at applied magnetic field. There is almost

immeasurable coercivity (0.614 Oe) for Fe_3O_4 at room temperature, this indicates that the Fe_3O_4 particles are superparamagnetic and nanosized. The saturation magnetization, M_s , are 60.1 emu/g for Fe_2O_3 , which are lower than that of bulk hematite particles ($M_{\text{bulk}} = 98 \text{ emu/g}$). From the magnetization curves it can be seen that the magnetization does not saturate for Fe_2O_3 and Fe_3O_4 , even at 20000 Oe.

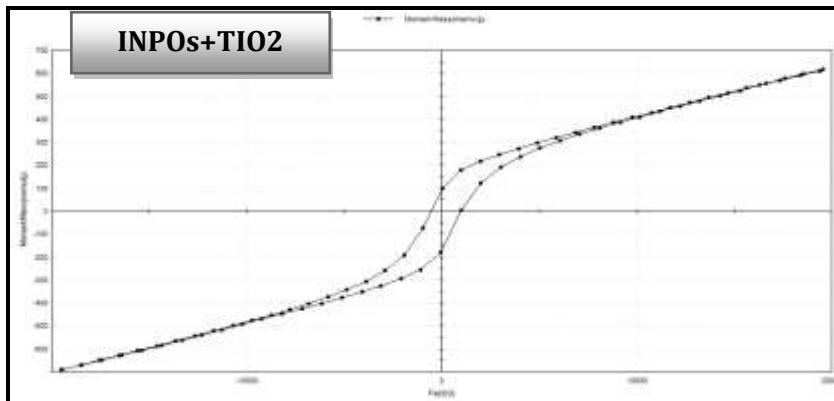


Fig. (8). Magnetization curves of iron oxide nanoparticles with composite TiO_2 -anatase.

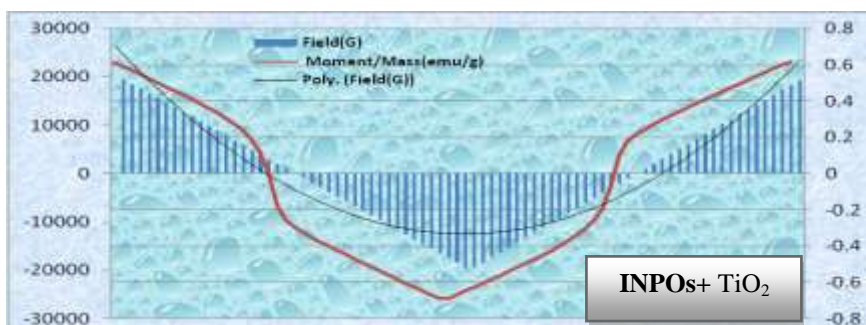


Fig. (9). Magnetization graph of iron oxide nanoparticles with composite TiO_2 - anatase.

3.5. Effect of nanocomposite iron/ TiO_2 particles on polluted wastewater

3.5.1. Removal of chromium and iron metals by magnetic nanocomposite by magnetic iron/ TiO_2 nanocomposite

Pollution of water is discussed on the basis of determining inorganic, biological, organic and bacteriological pollutants analyses with regard to the recommended level of contamination. The chemical inorganic pollutants of water samples in the studied area are discussed through the measurements of trace elements, heavy metals and minor ions. Table (1) shows elevated level of chromium and iron metals than permissible standard level. Before

treatment, the concentration of chromium in industrial wastewater was 0.0638 ppm (Table 1), which decreased to 0.0008 ppm (Table 2) after treatment with nanocomposite iron/ TiO₂ particles. This inhibition indicated that the adsorption efficiency of prepared nanoparticles composite had 98.74% as reduction percentage (Table 3) and the particles of composite had a nanosized shape with large surface area at optimal condition done. In case of sewage water station, as shown in table (1 and 2), the concentration of chromium was 0.0657 ppm before treatment and 0.005 ppm after treatment, that revealed a reduction percentage of 92.38% (Table 3). The iron concentration of industrial wastewater before treatment had an impermissible limit, but after treatment the range of iron as a toxic metal in water reached to 0.001 ppm (Table 2) from 0.9197 ppm (Table 1) with reduction percentage of 99.89% (Table 3). Also, the concentration of iron before treatment of sewage water station had an impermissible limit of 0.4747 ppm (Table 1), but after treatment reached to 0.007 ppm (Table 2) with reduction percentage of 98.99% (Table 3). The mechanism of action of removal of chromium ion depends on physical interaction (adsorption and desorption) between iron nanocomposite and chromium ions.

Table (1). Analysis of heavy metals (ppm) before treatment by nanoparticles.

Parameter	Permissible limit	Industrial wastewater 10th Ramadan	Sewage water 10th Ramadan
	-----	9.80 pH	6.86 pH
Aluminum	<0.200	0.1028	0.2041
Boron	<0.500	<0.0300	<0.0300
Barium	<0.200	0.0093	0.0325
Cadmium	<0.005	<0.0006	<0.0006
Cobalt	<0.050	<0.0010	<0.0010
Chromium	<0.050	0.0638	0.0657
Copper	<0.050	<0.0090	0.0513
Iron	<0.300	0.9179	0.4747
Manganese	<0.500	0.0243	0.0476
Molybdenum	<0.010	<0.0030	<0.0030
Nickel	<0.100	0.0351	0.0390
Lead	<0.050	<0.0060	<0.0060
Strontium	<0.500	0.1087	0.4805
Vanadium	<0.010	<0.0100	<0.0100
Zinc	<5.000	0.0267	0.1345

Table (2). Analysis of heavy metals (ppm) after treatment by nanoparticles.

Parameter	Permissible limit	Industrial wastewater 10 th Ramadan	Sewage water 10 th Ramadan
	-----	9.80 pH	6.86 pH
Aluminum	<0.200	0.0028	0.0204
Boron	<0.500	<0.0100	<0.0100
Barium	<0.200	0.0023	0.01250
Cadmium	<0.005	<0.0006	<0.0006
Cobalt	<0.050	<0.0010	<0.0010
Chromium	<0.050	0.0008	0.0050
Copper	<0.050	<0.0090	0.0110
Iron	<0.300	0.0010	0.0070
Manganese	<0.500	0.01130	0.0106
Molybdenum	<0.010	<0.0010	<0.0010
Nickel	<0.100	0.0010	0.0010
Lead	<0.050	<0.0060	<0.0060
Strontium	<0.50	0.0070	0.0015
Vanadium	<0.010	<0.0100	<0.0100
Zinc	<5.000	0.0067	0.0050

Table (3). Reduction percent of chromium and iron before and after treatment by synthesized nano iron oxide composite TiO₂ of polluted waters.

Location	Chromium ppm			Iron ppm		
	Before treatment	After treatment	Reduction %	Before treatment	After treatment	Reduction %
	0.0657	0.0050	92.38	0.5254	0.007	98.66
B	0.0638	0.0008	98.74	0.9179	0.001	99.89
Synthesized	40.3700	3.0000	92.56	64.5800	12.470	80.69

A: Sewage water 10th Ramadan B: Industrial wastewater 10th Ramadan

3.5.2. Removal of total nitrogen, nitrate and phosphates by magnetic iron/TiO₂ nanocomposite

Table (4) and Fig. (10) show the ability of magnetic nanocomposite iron/TiO₂ particles for removal of nitrogen group as a core of nitrate derivatives. The adsorption efficiency (reduction percentage) as total

nitrogen adsorbed on nanocomposite particles was 33.33 and 100% in case of nitrate groups adsorbed on nanocomposite particles in sewage water station. But, in case of industrial wastewater, the reduction percentage was 31.25% as total nitrogen adsorbed and 56.64% as nitrate adsorbed on nanocomposite particles. The mechanism of removal of nitrogen depends on formation of weak bonds between active site of hydroxyl group on nanocomposite with lone pair electrons of nitrogen.

Table (4). Reduction percentage of nitrate, total nitrogen and phosphate by nanoparticles before and after treatment of polluted wastewater.

Location	Total nitrogen (ppm)			Nitrate (ppm)			Phosphate (ppm)		
	Before treatment	After treatment	Reduction %	Before treatment	After treatment	Reduction %	Before treatment	After treatment	Reduction %
A	33.6	22.4	33.33	106.4	0.0	100	5.8	2.7	53.44
B	22.4	15.4	31.25	48.9	21.2	56.64	3.55	0.0	100

A: Sewage water 10th Ramadan B: Industrial wastewater 10th Ramadan

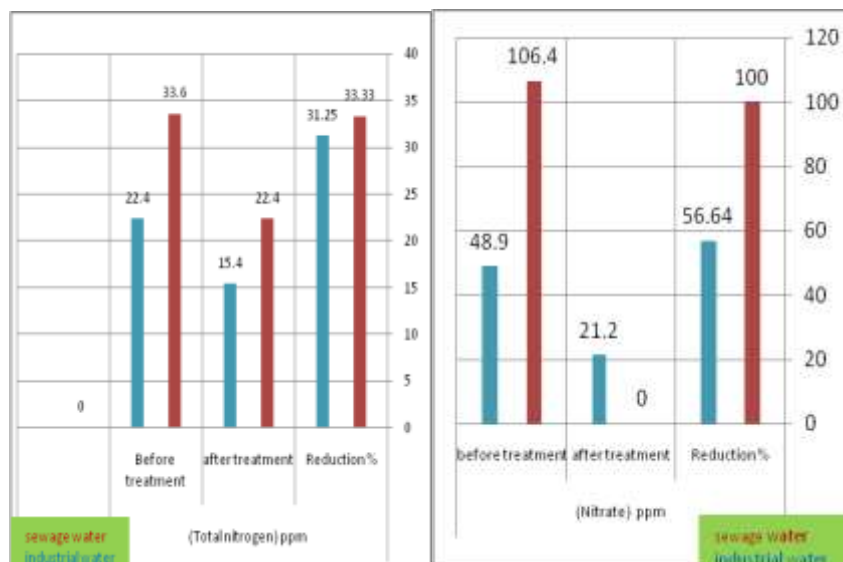


Fig. (10). Effect of nanocomposite iron/ TiO₂ on total nitrogen and nitrate group.

3.5.3. Removal of phosphate content by magnetic iron/TiO₂ nanocomposite

In table (4) and Fig. (11), the reduction percentage of phosphate content was 100 and 53.44% for sewage water and industrial wastewater, respectively. The decreasing of phosphate content was caused by increasing

of reduction percentage (adsorption efficiency) of nanocomposite iron/TiO₂ particles. The increasing of reduction percentage was caused by the increasing of adsorption and desorption (mechanism of reaction) of phosphate group on nanocomposite particles and largest molecular weight of phosphate group.

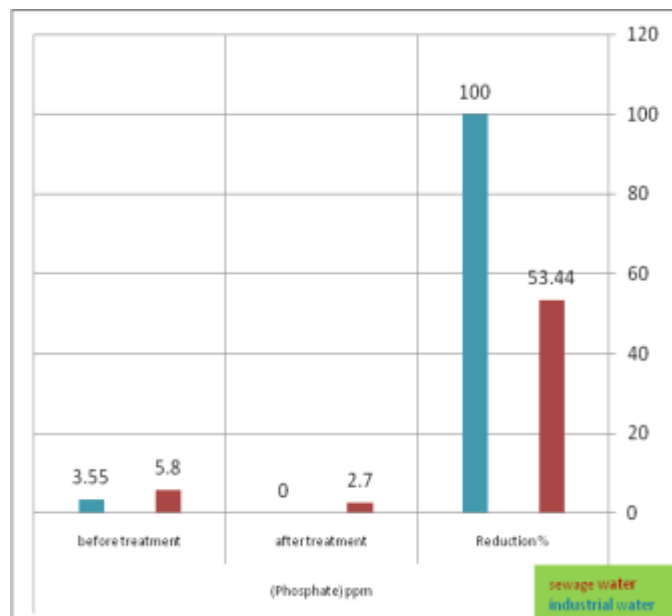


Fig. (11). Effect of nanocomposite iron/TiO₂ on phosphate group.

CONCLUSION

This study investigated the synthesis of super-paramagnetic iron oxide nanoparticles with TiO₂-anatase prepared by a co-precipitation method, using propylene glycol as surfactant. This was for the purpose of achievement for removal of chromium and iron metals as an inorganic pollutant in sewage water and industrial wastewater. Fourier transforms infrared spectra and X-ray diffraction showed that the iron oxides MNPs were successfully coated by TiO₂-anatase. The results showed that the crystallite and average particle size of the iron oxides MNPs coated by TiO₂-anatase were dependent on pH, temperature, sonication time and MNPs composite with TiO₂-anatase concentration. The saturation magnetization of the MNPs was proportional to the particle size. The present investigation showed that the nano-particles are effective adsorbents for the removal of iron and chromium ions from aqueous solutions. The adsorption process is a function of pH, reaction time, adsorbent concentration and temperature. The

efficiency of iron and chromium ions adsorption increases with increasing adsorbent dosage and temperature at certain limits.

REFERENCES

- Altundogan, H.S. (2005). Arsenic removal from aqueous solution by adsorption on red mud. *Process Biochemistry*, 40: 1443-1452.
- Booker, N.A., D. Keir, A.J. Priestley, C.B. Ritchie, D.L. Sudarmana and M.A. Woods (1991). Sewage clarification with magnetite particles, *Water Sci. Technol.*, 23: 1703-1712.
- Chang, Y.C. and D.H. Chen (2005). Preparation and adsorption properties of monodisperse chitosan-bound Fe₃O₄ magnetic nanoparticles for removal of Cu(II) ions. *J. Colloid Interface Sci.*, 283: 446–451.
- Cornell, R.M. and U. Schertmann (1991). *Iron Oxides in the Laboratory; Preparation and Characterization*. Weinheim, VCH.
- Gao, Y., Y. Masuda, Z. Peng, T. Yonezawa and K.J. Koumoto (2003). Room temperature deposition of a TiO₂ thin film from aqueous peroxotitanate solution, *J. Mater. Chem.*, 13: 608–613.
- Goh, P.S., B.C. Ng, W.J. Lau and A.F. Ismail (2015). Inorganic nano-materials in polymeric ultrafiltration membranes for water treatment. *Sep. Purif. Rev.*, 44: 216–249.
- Guo, L., G. Liu, R.Y. Hong and H.Z. Li (2010). Preparation and characterization of chitosan poly (acrylic acid) magnetic microspheres. *Marine Drugs*, 8: 2212–2222.
- Kang, Y.S., S.J. Risbud, F. Rabolt and P. Stroeve (1996). Synthesis and characterization of nanometer-size Fe₃O₄ and Fe₂O₃ particles, *Chem. Mater.*, 2209–2211.
- Mahdavi, M., F. Namvar, M.B. Ahmad and R. Mohamad (2007). Green biosynthesis and characterization of magnetic iron oxide (Fe₃O₄) nanoparticles using seaweed (*Sargassum muticum*) aqueous extract. *Moecules*, 18: 5954–596.
- Mahdavi, M., M.B. Ahmad, M.J. Haron, Y. Gharayebi, K. Shameli and B. Nadi (2013). Fabrication and characterization of SiO₂/(3-aminopropyl) triethoxysilane-coated magnetite nanoparticles for lead (II) removal from aqueous solution. *J. Inorg. Organomet. Polym.*, 23: 599–607.
- Ngomsik, A.F., A. Bee, M. Draye, G. Cote and V. Cabuil (2005). Magnetic nano- and microparticles for metal removal and environmental applications: a review, *Comptes Rendus Chimie*, 8: 963–970.
- Okuda, T., I. Sugano and T. Tsuji (1975). Removal of heavy metals from wastewater by ferrite co-precipitation. *Filtration and Separation*, 12: 475-476.

- Orbell, J.D., L. Godhino, S.W. Bigger, T.M. Nguyen and L.N. Ngeh (1997). Oil spill remediation using magnetic particles-an experiment in environmental technology. *J. Chem. Educ.*, 74: 1446-1448.
- Ouki, S.K. and R.D. Neufeld (1997). Use of activated carbon for the recovery of chromium from industrial wastewaters. *Journal of Chem. Tech. and Biotech.*, 70: 3-8.
- Pathak, A., A.B. Panda, A. Tarafdar and P. Pramanik (2003). Synthesis of nano-sized metal oxide powders and their application in separation technology. *J. Indian Chem. Soc.*, 80: 289-296.
- Pradhan, P., J. Giri, G. Samanta, H.D. Sarma, K.P. Mishra, J. Bellare, R. Banerjee and D. Bahadur (2006). Comparative evaluation of heating ability and biocompatibility of different ferrite-based magnetic fluids for hyperthermia application. *J. Biomed. Mater. Res.*, 81B: 12-22.
- Qu, J., G. Liu, Y. Wang and R. Hong (2010). Preparation of Fe₃O₄-chitosan nanoparticles used for hyperthermia. *Adv. Powder. Technol.*, 2: 461-467.
- Shen, Y.F., J. Tang, Z.H. Nie, Y.D. Wang, Y. Ren and L. Zuo (2009). Preparation and application of magnetic Fe₃O₄ nanoparticles for wastewater purification. *Sep. Purif. Technol.*, 68: 312-319.
- Sun, J., S. Zhou, P. Hou, Y. Yang, J. Weng, X. Li and M. Li (2006). Synthesis and characterization of biocompatible Fe₃O₄ nanoparticles. *J. Biomed. Mater. Res., Part A*, 10: 333-341.
- Tartaj, P., M.D. Morales, S. Veintemillas-Verdaguer, T. Gonzalez-Carreño and C.J. Serna (2003). The preparation of magnetic nanoparticles for applications in biomedicine. *J. Phys. D: Appl. Phys.*, 36: 182-197.
- Tartaj, P., M.D. Morales, S. Veintemillas-Verdaguer, T. Gonzalez-Carreño and C.J. Serna (2005). Advances in magnetic nanoparticles for biotechnology applications. *J. Magn. Magn. Mater.*, 290: 28-34.
- Warner, C.L., R.S. Addleman, A.D. Cinson, T.C. Droubay; M.H. Engelhard, M.A. Nash, W. Yantasee and M.G. Warner (2010). High-performance, superparamagnetic, nanoparticle-based heavy metal sorbents for removal of contaminants from natural waters, *ChemSusChem*, 3: 749-757.
- Zhao, X., L. Lv, B. Pan, W. Zhang, S. Zhang and Q. Zhang (2011). Polymer-supported nanocomposites for environmental application – a review. *Chem. Eng. J.*, 170 (2-3): 381-394.

التخلص من العناصر الثقيلة الذائبة لمياه الصرف باستخدام مركبات أكاسيد التيتانيوم/الحديد النانومغناطيسية بمنطقة العاشر من رمضان - مصر

مجدي حسني السيد وياسر عبدالمطلب عبد الهادي*

قسم الهيدروجيوكيميا، وحدة معالجة وتحلية المياه، مركز التميز المصري لأبحاث التحلية، مركز بحوث الصحراء، المطرية، القاهرة، مصر

يتناول البحث تحضير بعض المواد النانوية من أيون الحديد المغناطيسي والتي لها خواص مغناطيسية تستخدم في معالجة مياه الصرف بأنواعها المختلفة (الزراعي- الصحي- الصناعي) في المناطق الصحراوية والصناعية بمدينة العاشر من رمضان (منطقة الدراسة). ويستعرض البحث التجارب العملية لتحضير مركب الحديد المغناطيسي وأكسيد التيتانيوم بطريقة الترسيب الكيميائي وكذلك طريقة الإستحلاب الدقيق. يعتبر تحضير تلك المركبات ذات خواص مغناطيسية تساهم في إدمصاص العناصر الثقيلة (السامة) من مياه الصرف بالخاصية المغناطيسية. ووجود أيونات الحديد المغناطيسي كنواة نانوية مغلقة بأكسيد التيتانيوم يساعد على التخلص من الملوثات العضوية والغير عضوية والبيولوجية.

وقد تم دراسة المعاملات الكيميائية ذات التأثير المباشر على كفاءة الفصل العنصري للعناصر السامة في مياه الصرف للمواد النانوية، مثل دراسة تأثير الرقم الهيدروجيني ودرجة الحرارة وزمن الإهتزاز للمحلول النانوي مع العينة، وذلك للوصول إلى حجم نانوى صغير لزيادة مساحة سطح الإدمصاص للجزيئات النانوية. وقد إستخدم جهاز الميكروسكوب الماسح الإلكتروني في تصوير سطح الجزيئات النانوية وجهاز الأشعة تحت الحمراء لتحديد المجاميع الوظيفية لجزيئات النانو والتي لها دور كبير في إزالة الملوثات بأنواعها، وكذلك جهاز القدرة المغناطيسية للمواد النانوية المحضرة وجهاز الأشعة السينية لتحديد المركبات المستخدمة ونسب التكوين لجزيئات نانو الحديد المغناطيسية. وقد وصلت نسبة إزالة أيون الكروم وأيون الحديد (عناصر ثقيلة سامة) في مياه الصرف الصحي لمدينة العاشر من رمضان بمحافظة الشرقية باستخدام جزيئات الحديد المغناطيسي المغطى بأيونات أكسيد التيتانيوم إلى ٩٢.٣٨ - ٩٨.٦٦%. ووصلت نسبة إزالة نفس العنصرين إلى ٩٩.٨٩ - ٩٨.٧٤% في مياه الصرف الصناعي (الشركة الوطنية لمنتجات الذرة). وقد تناول البحث أيضًا إزالة بعض الملوثات الغيرعضوية كالنيتروجين الكلي ومجاميع النترات ومجاميع الفوسفات إلى ٣٣.٣٣، ١٠٠ و ٥٣.٤٤%، على التوالي، في مياه الصرف الصحي لمدينة العاشر من رمضان. كما وصلت نسبة إزالة الملوثات للنيتروجين الكلي والنترات والفوسفات في مياه الصرف الصناعي للشركة إلى ٣١.٢٥، ٥٦.٦٤ و ١٠٠%، على التوالي. وتوضح النتائج في نهاية البحث مدى كفاءة فصل وإدمصاص المواد النانوية المحضرة بطرق معملية بسيطة للعناصر السامة (الثقيلة) للملوثات العضوية. وإتضح ذلك في إزالة أيون الكروم السام ذي اللون الداكن وكذلك أيون الحديد والذي يعتبر من أهم الملوثات الثقيلة في المياه. وأيضًا إزالة الملوثات الغير عضوية كالنترات والفوسفات في مياه الصرف الزراعي بشكل خاص بنسب كبيرة. وجاري متابعة وإستكمال البحوث في هذا الإطار للوصول لمعدلات تنقية ومعالجة لمياه الصرف بكافة أنواعه بنسب مقبولة وفي الحدود المسموح بها طبقًا للمواصفة العالمية والمواصفة القياسية المصرية.